JACS
JOURNAL OF THE AMERICAN CHEMICAL SOCIETY

Communication

pubs.acs.org/JACS

Controlling Formation of Single-Molecule Junctions by Electrochemical Reduction of Diazonium Terminal Groups

Thomas Hines,[†] Ismael Díez-Pérez,[‡] Hisao Nakamura,[§] Tomomi Shimazaki,[⊥] Yoshihiro Asai,[§] and Nongjian Tao*,[†]

[†]Center for Biosensors and Bioelectronics, The Biodesign Institute, and School of Electrical, Computer and Energy Engineering, Arizona State University, Tempe, Arizona 85287, United States

[‡]Department of Physical Chemistry, University of Barcelona & Institute for Bioengineering of Catalonia, Barcelona 08028, Spain

[⊥]RIKEN Advanced Institute for Computational Science, 7-1-26, Minatojima-minami-machi, Chuo-ku, Kobe 650-0047, Japan

[§]Nanosystem Research Institute "RICS", National Institute of Advanced Industrial Science and Technology, Umezono 1-1-1, Tsukuba Central 2, Tsukuba, Ibaraki 305-8568, Japan

Supporting Information

ABSTRACT: We report controlling the formation of single-molecule junctions by means of electrochemically reducing two axialdiazonium terminal groups on a molecule, thereby producing direct Au−C covalent bonds *in situ* between the molecule and gold electrodes. We report a yield enhancement in molecular junction formation as the electrochemical potential of both junction electrodes approach the reduction potential of the diazonium terminal groups. Step length analysis shows that the molecular junction is significantly more stable, and can be pulled over a longer distance than a comparable junction created with amine anchoring bonds. The stability of the junction is explained by the calculated lower binding energy associated with the direct Au−C bond compared with the Au−N bond.

The anchoring of a molecule to a metal surface is a key factor that affects both charge transport and stability in single-molecule junctions.[1] Anchoring is usually achieved by using one of several linker groups that covalently bond the molecule to the electrodes. Thiols[2,3] and amines[3,4] have been characterized extensively in the literature; while other reported linkers include pyridine,[5] isocyanide,[6] nitrile,[7] carbodithiolate,[8] and carboxyl[3] groups. Additionally molecular junctions formed by direct Au−C covalent bonds were reported by cleaving trimethyltin terminal groups,[9,10] trimethyl silyl groups,[11] and by bonding fullerenes directly to gold.[12,13] However, in all of these cases the energetics of bond formation is invariant to the surrounding environment. Thus, the only way to control formation and rupture of the junction is by mechanically manipulating electrodes, either through a mechanically controlled break junction[14,15] or scanning tunneling microscope (STM) break junction.[2]

An alternative approach of binding molecules to electrodes utilizes the electrochemical reduction of a diazonium ion placed at the terminal end of a linear molecule.[16] This process allows control over the binding energetics of deposition via manipulation of an externally controlled electrochemical gate. Upon reduction, the terminal diazonium ion is cleaved from backbone of the molecule creating an aryl radical. The radical then reacts with a carbon or metal electrode by forming a direct covalent bond with uninterrupted π conjugation.[16−22] The nature of this bond has been verified using Raman[23,24] and X-ray photoelectron spectroscopy.[23,25] McCreery et al. have employed this process to graft thousands of molecules to carbon electrodes so that they may be used as active components in hybrid devices fabricated by using conventional CMOS techniques.[26−30] This diazonium reduction process produced a more compact and robust organic layer than was achievable using conventional covalent linker groups, which reduced diffusion of metallic species from top coats deposited by thermal evaporation.[27]

Here we apply the electrochemical reduction of diazonium groups to the STM break junction process, thereby allowing electrochemical control over the formation of a stable single molecule junction. We use a biphenyl molecule with ortho placed methoxy groups and axially placed diazonium terminal groups on either end. Calculations presented in Table S1 show that the methoxy groups do not have a significant effect on either the assembly process or the conductance of the molecule. The structure of this molecule differs from molecules used in hybrid devices because in this case the diazonium ions are placed at both ends of the molecule. As a result, setting the electrochemical potential to the reduction potential of the diazonium ion induces formation of a metal−molecule−metal junction directly connected by Au−C bonds. By mechanically breaking the junction, the formation and breaking process may be repeated a finite number of times. Furthermore, we show that the molecule electrode coupling created by the direct Au−C bonding produces a significantly more robust junction than in the same molecule connected using amine linkers.

Molecular junctions were formed using the STM break junction technique.[2] The STM used to carry out experiments was equipped with a bipotentiostat that allowed electrochemical control of the diazonium reaction. With this setup, a solution of ~2 mM 2,2′-dimethoxybiphenyl-4,4′-bis(diazonium) zinc tetrachloride (Sigma-Aldrich, 95% and referred to as **bp1** from this

Received: November 6, 2012
Published: February 13, 2013

   dx.doi.org/10.1021/ja3106434 | *J. Am. Chem. Soc.* 2013, 135, 3319−3322

point forward) was dissolved in anhydrous acetonitrile with 25 mM tetrabutylammonium hexafluorophosphate ($TBAPF_6$) and added dropwise to the STM cell filled with the electrolyte at open-circuit potential. The cyclic voltamogram shown in Figure 1 displays successive scans in green (1st cycle) and red (2nd

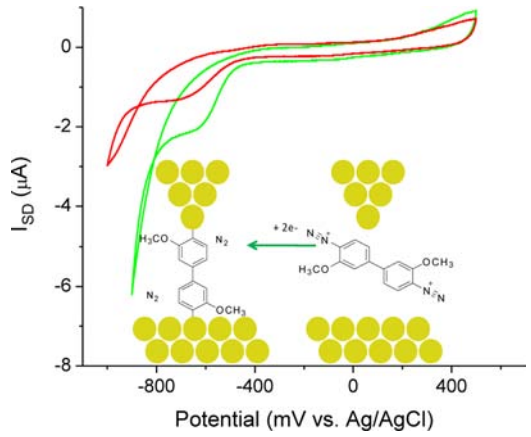

Figure 1. Cyclic voltamogram of the **bp1** molecule used in experiments. The diazonium terminal groups were irreversibly reduced at ~ −650 mV vs Ag/AgCl.

cycle) showing a prominent reduction peak at ~ −650 mV vs Ag/AgCl. As illustrated in the inset schematic, this potential corresponds to the reduction of the diazonium linker groups, and deposition of the **bp1** molecule directly onto the gold electrode via a Au−C covalent bond.[17,20] Also noteworthy is the lack of any corresponding oxidation peak, and the surface passivation observed by the peak intensity decrease in successive cycles, showing that the reaction is irreversible and the backbone of the molecule is electrochemically inactive.

Conductance traces for **bp1** were recorded by repeatedly bringing a gold STM tip into and out of contact with the gold substrate with the sample-tip bias fixed at 20 mV and electrochemical potential applied to both electrodes. When the tip was retracted in the absence of molecules binding to the electrodes, a clean exponential decay in the current was recorded within the conductance range below G_0. However when a molecular bridge was formed a plateau was recorded in the current decay curve, which corresponded to the approximate current measured through a single molecule junction. Due to the irreversible nature of the diazonium electrochemical reduction, conductance traces were recorded starting 0 mV applied potential (vs Ag/AgCl) and the electrochemical potential was successively decreased in intervals of 100 mV until reaching the potential of the diazonium reduction reaction. The experiment was carried out on four separate occasions. Conductance traces were compiled into conductance histograms and are shown in Figure 2. The histograms were compiled by applying the same automated selection criteria to each set of recorded decay curves. In this process, traces showing counts exceeding a defined threshold at conductance values within a given interval range were added to the conductance histogram. This selection process made peaks in the conductance histograms more prominent above the tunneling background and also allowed a quantitative measure of the yield of molecular junction formation in all of the conductance traces. The conductance histograms in Figure 2 show that between 0 and −200 mV vs Ag/AgCl, a conductance peak is not noticeable above the tunneling background. This is

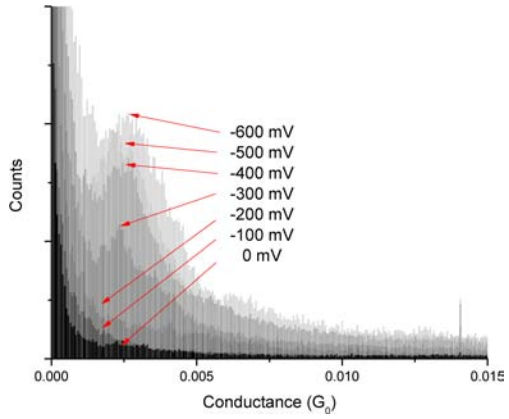

Figure 2. Conductance histograms in linear scale taken at electrochemical potentials ranging from 0 to −600 mV vs Ag/AgCl. Conductance peaks appeared at −300 mV and below, indicating that single-molecule junction formation occurs near the reduction potential of the diazonium groups.

attributed to the relatively low yield of molecular junction formation at these electrochemical potentials compared to the inevitable "false counts" that result from employing automated selection criteria. However, when the electrochemical potential is decreased to −300 mV vs Ag/AgCl and below, conductance histograms show a prominent peak centered at ~2.3×10^{-3} G_0.

A plot of measured conductance of **bp1** as a function of applied electrochemical potential vs Ag/AgCl is presented in Figure 3a. Median and standard deviation of conductance were

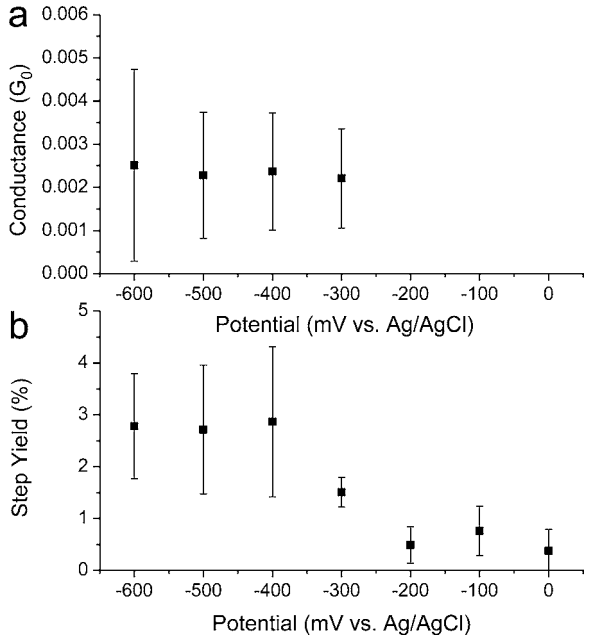

Figure 3. (a) Conductance peaks extracted from Figure 2 as a function of applied electrochemical potential. (b) Relative yield of forming a molecular junction as a function of applied electrochemical potential.

found by fitting each peak presented in Figure 2 to a Gaussian distribution. Those histograms that did not show any prominent peaks were not fitted and thus are not represented in Figure 3a. It is evident that once the two-diazonium linker groups are reduced to form a molecular junction, the measured conductance is relatively invariant to the applied electro-

dx.doi.org/10.1021/ja3106434 | J. Am. Chem. Soc. 2013, 135, 3319−3322

chemical potential. This is supported by the fact that the CV shown in Figure 1 does not show any electrochemical activity associated with the biphenyl backbone of the molecule.

The yield of molecular junction formation for **bp1** was found by applying the same automated selection criteria to each set of conductance decay curves collected at different electrochemical potentials. Yield is defined as the number of transient decay curves showing steps divided by the total number of decay curves collected. Thus, the yield serves as a measure of the tendency of a molecular junction to form. Figure 3b shows the weighted mean yield of molecular junction formation, along with standard deviation, recorded across four different experiments. For applied electrochemical potentials between 0 and −200 mV vs Ag/AgCl the data shows relatively low single-molecule junction formation, on average below 1%, which correlates with the lack of any apparent peaks in the corresponding conductance histograms. However when the applied electrochemical potential is set to −300 mV and below, step yield noticeably increases to between 1% and 5%. This trend shows a direct correlation between the applied electrochemical potential and the formation of single-molecule junctions, which supports the conclusion that the molecular junction is forming by electrochemical reduction of the diazonium terminal groups.

To determine the role that the Au−C covalent bond plays in the conductance and stability of the molecular junction, STM break junction measurements were also performed on 3,3′-dimethoxybenzidine (Sigma-Aldrich, and referred to as **bp2** from this point forward). **bp2** has the same backbone structure with ortho placed methoxy groups as **bp1** but has axially placed amine linkers instead of diazonium terminal groups (see inset of Figure 4b for schematic). Thus, **bp2** molecule acted as a control to the measurements taken with **bp1**. Previous reports of molecular junctions created by direct Au−C bonds by Venkataraman et al. reported up to a 100× increase in conductance compared to analogous molecular junctions bound by covalent amine bonds.[9,10] Conductance traces for **bp2** were recorded under the same bias conditions and in the same electrolyte as **bp1**; however the electrochemical potential was fixed at 0 mV vs Ag/AgCl because neither the backbone nor the amine linker groups of **bp2** are electrochemically active within the electrochemical working range. The conductance histogram for **bp2** (Figure S2) shows a median conductance of 1.4×10^{-3} G_0, meaning that the **bp1** junction is only 60% more conductive than **bp2**. Thus we see that despite previous reports of significantly higher conductance due to direct Au−C bonds, the measured conductances of the diazonium-terminated **bp1** and amine-terminated **bp2** molecules are fairly similar.

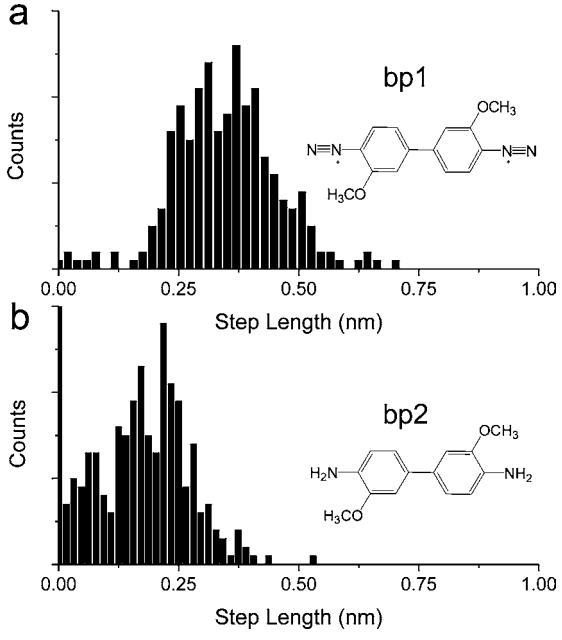

Figure 4. Step length histograms for **bp1** (a) and **bp2** (b). The stronger Au−C bond created in bp1 results in a junction that can be pulled almost twice as far as the amine terminated bp2.

The stretching distance of molecular junctions created with **bp1** and **bp2** was measured and plotted as step length histograms in Figure 4. Gaussian distributions were fitted to both histograms and show that the median pulling length for **bp1** is 0.34 nm, while for **bp2** it is much shorter, only 0.18 nm. This is the case despite the fact that the **bp1** junction measures 1.13 nm from Au apex to Au apex, compared to 1.34 nm for the **bp2** junction, which is longer because it contains intermediate amines between the phenyl rings and gold contacts. The longer pulling distance associated with the **bp1** junction can be attributed to the direct Au−C bond, which created a stronger bond with the gold electrode than the amine bond used in the **bp2** junction.

To complement the measured conductance and step length data for both molecules, density functional theory (DFT) and non-equilibrium Green's function transmission calculations were performed (details for which can be found in the Supporting Information).[31,32] Relevant data for these calculations is summarized in Table 1. Optimized junction geometries for both molecules showed that **bp1** had a much lower binding energy to the gold electrode than **bp2**, specifically −2.695 eV for **bp1** compared with −0.252 eV for **bp2**. This trend fits well with the step length histograms given in figure 4, because the more stable binding energetics of the Au−C bonding in **bp1** will give rise to a junction that can be pulled over a longer distance compared to the **bp2** counterpart. The calculations also show that the coupling of the conducting pi-orbital to the contacts is far lower for **bp1** (0.057 eV) compared to **bp2** (0.095 eV). We believe that this difference accounts for the fact that there is a relatively small difference in measured conductance between **bp1** and **bp2** compared to other side by side comparisons of Au−C and Au−N bonding schemes. Venkataraman et al. reported large differences—up to 100×—in conductance values between Au−C bonds and Au−N bonds in sigma dominated alkanes[9] and pi dominated xylylenes.[10] In both of these systems the direct Au−C bond resulted in strong coupling between the electrodes and the conducting orbital; however in the case of our system, the Au−C bond of **bp1** results in relatively weak coupling between the

Table 1. Binding Energies, Couplings, and Conductance Values Calculated for bp1 and bp2 Using Non-equilibrium Green's Function Combined with Density Functional Theory[a]

	E_{ads}	$\Gamma_{\pi^*\text{-electrode}}$	G_{calc}	G_{meas}
bp1	−2.695 eV	0.057 eV	0.016 G_0	2.3×10^{-3} G_0
bp2	−0.252 eV	0.095 eV	0.010 G_0	1.4×10^{-3} G_0

[a]Further details regarding calculations can be found in the Supporting Information.

dx.doi.org/10.1021/ja3106434 | J. Am. Chem. Soc. 2013, 135, 3319−3322

electrode and pi-orbital compared to that seen in **bp2**. Additionally, calculated conductance values confirm that **bp1** has only marginally higher conductance than **bp2**. In fact, the values in table 1 show that the calculated conductance of **bp1** (1.6×10^{-2} G_0) is only 60% greater than **bp2** (1.0×10^{-2} G_0), which is the same ratio observed between measured values for **bp1** and **bp2**. Since DFT often underestimates the energy gap of the highest occupied molecular orbital (HOMO) and lowest unoccupied molecular orbital (LUMO), it is difficult to compare the absolute values of calculated and observed conductance.[25] The error can be partially corrected by a GW calculation; however significantly longer computation time would be required.[26] In the present study, our focus in the calculations is to give a qualitative comparison between anchoring and conductance. Transport calculations followed by DFT are sufficient to estimate the electronic coupling and identify the conducting orbitals, and our results of **bp1** and **bp2** are reasonable.

In summary, we have demonstrated a method of controlling the formation of a single molecule junction by electrochemically reducing diazonium terminal groups to form direct Au−C bonds between the molecule and gold electrodes. The relative yield of junction formation increased as the electrochemical potential was lowered close to the reduction potential of the diazonium groups. Side-by-side comparison of the molecular junction formed by diazonium reduction (**bp1**) with a control junction formed by amine linkers (**bp2**) shows that **bp1** can be stretched significantly farther than **bp2**, but only has marginally higher conductance. This is explained in light of the fact that while **bp1** creates a stronger bond with the electrode, it has relatively weak coupling between the conducting orbital and electrodes compared to that seen in **bp2**.

■ ASSOCIATED CONTENT

Supporting Information

UV−vis spectroscopy data, additional conductance histograms, and theoretical calculations details. This material is available free of charge via the Internet at http://pubs.acs.org.

■ AUTHOR INFORMATION

Corresponding Author

njtao@asu.edu

Notes

The authors declare no competing financial interest.

■ ACKNOWLEDGMENTS

The work is supported by National Science Foundation (CHE-1105588, CHE-0931466, and ECS-0925498). I.D.-P. thanks the Ramon y Cajal program from MICINN and the EU International Reintegration Grant (FP7-PEOPLE-2010-RG-277182) for financial support.

■ REFERENCES

(1) Nitzan, A.; Ratner, M. A. *Science* **2003**, *300*, 1384.
(2) Xu, B. Q.; Tao, N. J. J. *Science* **2003**, *301*, 1221.
(3) Chen, F.; Li, X. L.; Hihath, J.; Huang, Z. F.; Tao, N. J. *J. Am. Chem. Soc.* **2006**, *128*, 15874.
(4) Venkataraman, L.; Klare, J. E.; Tam, I. W.; Nuckolls, C.; Hybertsen, M. S.; Steigerwald, M. L. *Nano Lett.* **2006**, *6*, 458.
(5) Xu, B. Q.; Xiao, X. Y.; Tao, N. J. *J. Am. Chem. Soc.* **2003**, *125*, 16164.
(6) Kiguchi, M.; Miura, S.; Hara, K.; Sawamura, M.; Murakoshi, K. *Appl. Phys. Lett.* **2006**, *89*, XXXX.
(7) Mishchenko, A.; Zotti, L. A.; Vonlanthen, D.; Burkle, M.; Pauly, F.; Cuevas, J. C.; Mayor, M.; Wandlowski, T. *J. Am. Chem. Soc.* **2011**, *133*, 184.
(8) Xing, Y. J.; Park, T. H.; Venkatramani, R.; Keinan, S.; Beratan, D. N.; Therien, M. J.; Borguet, E. *J. Am. Chem. Soc.* **2010**, *132*, 7946.
(9) Cheng, Z. L.; Skouta, R.; Vazquez, H.; Widawsky, J. R.; Schneebeli, S.; Chen, W.; Hybertsen, M. S.; Breslow, R.; Venkataraman, L. *Nature Nanotechnol.* **2011**, *6*, 353.
(10) Chen, W. B.; Widawsky, J. R.; Vazquez, H.; Schneebeli, S. T.; Hybertsen, M. S.; Breslow, R.; Venkataraman, L. *J. Am. Chem. Soc.* **2011**, *133*, 17160.
(11) Hong, W.; Li, H.; Liu, S.-X.; Fu, Y.; Li, J.; Kaliginedi, V.; Decurtins, S.; Wandlowski, T. *J. Am. Chem. Soc.* **2012**, *134*, 19425.
(12) Martin, C. A.; Ding, D.; Sorensen, J. K.; Bjornholm, T.; van Ruitenbeek, J. M.; van der Zant, H. S. J. *J. Am. Chem. Soc.* **2008**, *130*, 13198.
(13) Leary, E.; Gonzalez, M. T.; van der Pol, C.; Bryce, M. R.; Filippone, S.; Martin, N.; Rubio-Bollinger, G.; Agrait, N. *Nano Lett.* **2011**, *11*, 2236.
(14) Reed, M. A.; Zhou, C.; Muller, C. J.; Burgin, T. P.; Tour, J. M. *Science* **1997**, *278*, 252.
(15) Park, J.; Pasupathy, A. N.; Goldsmith, J. I.; Chang, C.; Yaish, Y.; Petta, J. R.; Rinkoski, M.; Sethna, J. P.; Abruna, H. D.; McEuen, P. L.; Ralph, D. C. *Nature* **2002**, *417*, 722.
(16) Ranganathan, S.; Steidel, I.; Anariba, F.; McCreery, R. L. *Nano Lett.* **2001**, *1*, 491.
(17) Allongue, P.; Delamar, M.; Desbat, B.; Fagebaume, O.; Hitmi, R.; Pinson, J.; Saveant, J. M. *J. Am. Chem. Soc.* **1997**, *119*, 201.
(18) Anariba, F.; DuVall, S. H.; McCreery, R. L. *Anal. Chem.* **2003**, *75*, 3837.
(19) Lehr, J.; Williamson, B. E.; Flavel, B. S.; Downard, A. J. *Langmuir* **2009**, *25*, 13503.
(20) Laforgue, A.; Addou, T.; Belanger, D. *Langmuir* **2005**, *21*, 6855.
(21) Bousquet, A.; Ceccato, M.; Hinge, M.; Pedersen, S. U.; Daasbjerg, K. *Langmuir* **2011**, *28*, 1267.
(22) Stockhausen, V.; Ghilane, J.; Martin, P.; Trippe-Allard, G.; Randriamahazaka, H.; Lacroix, J. C. *J. Am. Chem. Soc.* **2009**, *131*, 14920.
(23) Nowak, A. M.; McCreery, R. L. *Anal. Chem.* **2004**, *76*, 1089.
(24) Nowak, A. M.; McCreery, R. L. *J. Am. Chem. Soc.* **2004**, *126*, 16621.
(25) Mahmoud, A. M.; Bergren, A. J.; McCreery, R. L. *Anal. Chem.* **2009**, *81*, 6972.
(26) McCreery, R. L.; Wu, J.; Kalakodimi, R. P. *Phys. Chem. Chem. Phys.* **2006**, *8*, 2572.
(27) Ru, J.; Szeto, B.; Bonifas, A.; McCreery, R. L. *ACS Appl. Mater. Interfaces* **2010**, *2*, 3693.
(28) Bergren, A. J.; Harris, K. D.; Deng, F. J.; McCreery, R. L. *J. Phys.-Condensed Matter* **2008**, *20*, XXXX.
(29) Bonifas, A. P.; McCreery, R. L. *Nature Nanotechnol.* **2010**, *5*, 612.
(30) Martin, P.; Della Rocca, M. L.; Anthore, A.; Lafarge, P.; Lacroix, J. C. *J. Am. Chem. Soc.* **2012**, *134*, 154.
(31) Nakamura, H.; Yamashita, K.; Rocha, A. R.; Sanvito, S. *Phys. Rev. B* **2008**, *78*, XXXX.
(32) Nakamura, H.; Asai, Y.; Hihath, J.; Bruot, C.; Tao, N. J. *J. Phys. Chem. C* **2011**, *115*, 19931.